PERGAMON

International Journal of Rock Mechanics and Mining Sciences 36 (1999) 719–729

International Journal of Rock Mechanics and Mining Sciences

www.elsevier.com/locate/ijrmms

A two-dimensional linear variation displacement discontinuity method for three-layered elastic media

Keh-Jian Shou[a,*], J.A.L. Napier[b]

[a]Department of Civil Engineering, National Chung-Hsing University, 250 Kuo-Kuang Road, Taichung 402, Taiwan
[b]Division of Mining Technology, CSIR, P.O. Box 91230, Auckland Park 2006, Johannesburg, South Africa

Accepted 17 March 1999

Abstract

A new displacement discontinuity method is developed for the analysis of multi-layered elastic media. This approach is based on a novel superposition scheme and the analytical solution to the problem of a displacement discontinuity element within bonded half-planes. A three-layered elastic region is obtained by superposing two sets of bonded half-planes and subtracting one infinite plane. The advantages of this approach are: (1) it is not necessary to introduce elements at the interface, (2) the method is applicable for three dimensional modelling and (3) it can be extended to an N ($N>3$) layer system easily. The accuracy of the model is illustrated by comparing the numerical results with the analytical solutions for a hole in an infinite strip in tension and with the numerical solution for a pressurized crack within a three-layered system. In order to show the efficacy of the developed model, the simulation results of a typical South African mining problem and general tunnel excavation problems are also presented.

1. Introduction

Boundary element models are widely used in geomechanic problems for computing stresses and displacements around underground excavations. Most of these models assume the rock mass to be a homogeneous, isotropic, linearly elastic solid, although inhomogeneity and anisotropy can also be analyzed by the boundary element method [1–3]. An important development of the boundary element approach is that half-plane and bonded half-plane problems can be solved without making additional numerical approximations [2,4,5]. Problems involving layers of finite thickness are more difficult to treat as closed form fundamental singularity solutions are difficult to derive. The fundamental solution for a multi-layered medium can be derived using the Fourier Transformation method, but the solution contains improper integrals which must be calculated numerically [6–12].

Many important rock engineering problems involve analysis of the stress fields of multi-layered systems. For the problem of mining a tabular orebody with different hangingwall and footwall, in order to understand the potential instability in relation to the material contrast, it is necessary to consider the problem as a layered system composed of formations with different material properties. A stope approaching a dyke with different properties from the host rock, which may trigger slip along the interface or may induce seismic activity related to rockburst, is another typical problem involving material contrast and interface. Similarly, in the hydraulic fracturing operation for enhanced oil recovery, the material contrast and the existence of interface(s) play important roles on the behaviour of the man-made hydraulic fracture propagation. Assembling appropriate numerical techniques, capable of representing holes and cracks in a layered system, is essential for those problems.

The objective of this study is to develop a two-dimensional displacement discontinuity method for the

* Corresponding author. Tel.: +886-4-285-0989; fax: +886-4-286-2857.
E-mail address: kjshou@dragon.mchu.edu.tw (K.J. Shou)

0148-9062/99/$ - see front matter
PII: S0148-9062(99)00042-X

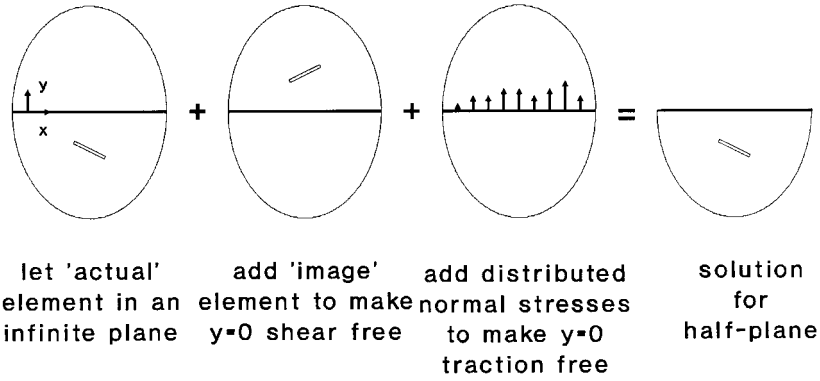

Fig. 1. Steps to obtain half-plane solution.

stress analysis of multi-layered elastic media. This approach is based on the principle of superposition and the analytical solution to the problem of a displacement discontinuity element within one of two perfectly bonded half-planes. A three-layered elastic region is obtained by superposing two different bonded half-plane regions. The advantages of this approach are: (1) it is not necessary to introduce elements at the interface, (2) the method is applicable for three dimensional modelling and (3) it can be extended to an N ($N>3$) layer system easily. The derivation of the superposition scheme for a general N ($N>3$) layer system will be presented in another paper.

2. Fundamental solution

In order to demonstrate more clearly the establishment of the fundamental solution for a displacement discontinuity element in a three-layer medium, the solution for a displacement discontinuity element in an infinite plane, a half-plane and bonded half-planes are presented briefly for completeness.

2.1. Solution for an infinite plane

The solution for the displacements and stresses at a point $(x,\ y)$ due to displacement discontinuity (D_x, D_y) over the line segment $|x|\le a,\ y=0$, can be expressed as

$$\begin{aligned}
u_x &= [2(1-\nu)f_{x,y} - yf_{x,xx}] + [-(1-2\nu)f_{y,x} - yf_{y,xy}]\\
u_y &= [(1-2\nu)f_{x,x} - yf_{x,xy}] + [2(1-\nu)f_{y,y} - yf_{y,yy}]\\
\sigma_{xx} &= 2G[2f_{x,xy} + yf_{x,xyy}] + 2G[f_{y,yy} + yf_{y,yyy}]\\
\sigma_{yy} &= 2G[-yf_{x,xyy}] + 2G[f_{y,yy} - yf_{y,yyy}]\\
\sigma_{xy} &= 2G[f_{x,yy} + yf_{x,yyy}] + 2G[-yf_{y,xyy}]
\end{aligned} \tag{1}$$

where

$$f_i(x,\ y) = \frac{-1}{4\pi(1-\nu)}\int_{-a}^{a} \mathrm{D}_i(\xi)\ln\sqrt{(x-\xi)^2+y^2}\,\mathrm{d}\xi \qquad i = x,\ y, \tag{2}$$

G is the shear modulus and ν is Poisson's ratio.

In the original displacement discontinuity formulation, i.e. the constant strength element presented by Crouch [13], the mid-element stresses and displacements were assumed to adequately represent the effective values over the length of the discontinuity. For the linear variation element, with four degrees of freedom, two nodes within the discontinuity must be chosen at which the representative measures of stresses and displacements are evaluated. In this study, the two Gauss–Chebyshev integration points (at $x=\pm a/\sqrt{2},\ y=0$) are used [14] and the local displacement discontinuity components can be expressed as

$$D_i(\xi) = N_1(\xi)D_i(1) + N_2(\xi)D_i(2) \quad i = x,\ y \tag{3}$$

where

$$N_1(\xi) = \frac{1}{2} - \frac{\xi}{\sqrt{2}} \qquad N_2(\xi) = \frac{1}{2} + \frac{\xi}{\sqrt{2}} \tag{4}$$

and $D_i(j)$ ($i=x,\ y$ and $j=1,\ 2$) are the nodal displacement discontinuities.

2.2. Solution for a half-plane

The fundamental solution for a constant strength displacement discontinuity element in a semi-infinite region y $\le$ 0 can be obtained by using the method of images [2,15]. Based on the principle of superposition, the method of images can be used to find the solution of the problem in two steps. In the first step, consider a displacement discontinuity element, the 'actual' element, in the region $y<0$ and suppose that a second element representing its 'image', reflected about $y=0$, exists in $y>0$. By symmetry, this setting ensures zero shear traction on $y=0$, however, the normal traction is not zero. In the second step, a supplementary sol-

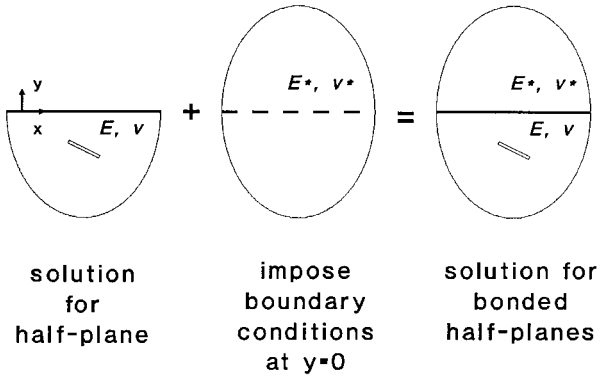

Fig. 2. Steps to obtain the bonded half-plane solution.

ution, related to a prescribed normal traction on $y = 0$, is obtained to make the normal traction vanish (see Fig. 1). Therefore, the complete solution for the half-plane $y \leq 0$ can be written as:

$$u_i = (u_i)_A + (u_i)_I + (u_i)_S$$
$$\sigma_{ij} = (\sigma_{ij})_A + (\sigma_{ij})_I + (\sigma_{ij})_S \quad (5)$$

where subscripts A, I, and S denote the displacements and stresses due to the actual element, the image element and the supplementary solution.

2.3. Solution for bonded half-planes

For a displacement discontinuity element within bonded half-planes, the fundamental solution can be obtained by the method of images with one more step (see Fig. 2) to the half-plane solution. This is accomplished by introducing a general form of solution u_i^* and σ_{ij}^* for the upper half-plane and an additional supplementary solution u_i^{**} and σ_{ij}^{**} for the lower half-plane. Superposing the lower and upper half-planes, the induced boundary conditions at the surface $y = 0$, which ensure that the stresses and displacements are continuous at the interface are as follows:

$$u_x = u_x^* \qquad u_y = u_y^* \qquad \sigma_{xy} = \sigma_{xy}^*$$
$$\sigma_{yy} = \sigma_{yy}^* \quad \text{for} \quad -\infty < x < \infty, \; y = 0 \quad (6)$$

where

$$u_i = (u_i)_A + (u_i)_I + (u_i)_S + u_i^{**}$$
$$\sigma_{ij} = (\sigma_{ij})_A + (\sigma_{ij})_I + (\sigma_{ij})_S + \sigma_{ij}^{**} \quad (7)$$

is the complete solution for the half-plane $y \leq 0$ and where u_i^{**} and σ_{ij}^{**} represent the displacement and stress components in the lower half-plane due to the stresses applied to the negative side of the interface $y = 0^-$. The complete solution for the upper half-plane is u_i^* and σ_{ij}^*, which depends only upon the normal and shear stresses applied to the positive side of the interface $y = 0^+$. Based on the theory of elasticity [16], the solutions u_i^{**}, σ_{ij}^{**}, u_i^* and σ_{ij}^* can be expressed in terms of displacement potential functions. We can derive these potential functions by considering the continuity conditions specified by Eq. (6). The solutions u_i and σ_{ij} can be obtained by introducing the terms u_i^{**} and σ_{ij}^{**} in Eq. (7).

2.4. Solution for a three-layer medium

In this study, the solution of a displacement discontinuity element within a three-layer medium was derived by a superposition procedure, which is based on the appropriate combination of appropriate bonded half-plane solutions. In particular, a three-layered elastic region, with Young's moduli E_1, E_2 and E_3, can be obtained by superposing two sets of bonded half-plane regions and an infinite plane. This is accomplished by introducing two sets of bonded half-plane solutions with different elastic modulus sets (E_2, E_3) and (E_1, E_2) and subtracting a supplementary infinite domain solution, as shown in Fig. 3. The complete solution can

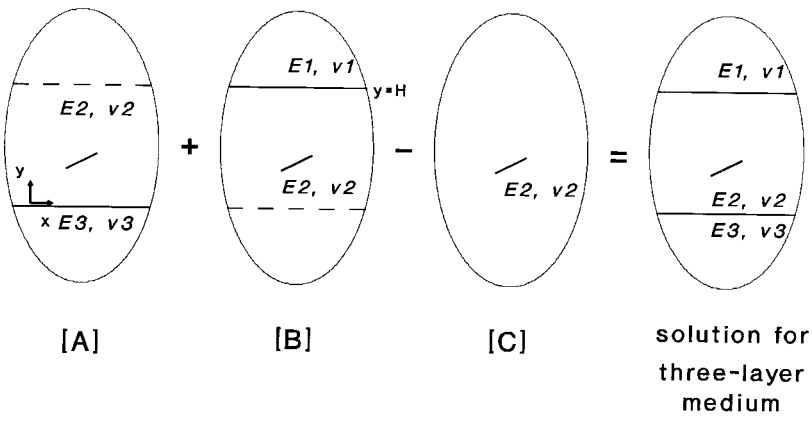

Fig. 3. Steps to obtain solution for a three-layered medium.

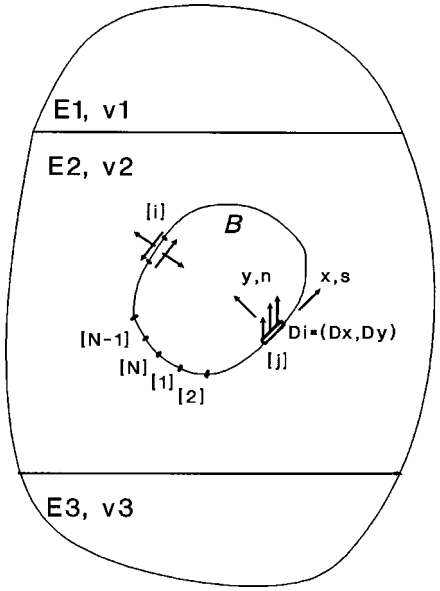

Fig. 4. Displacement discontinuity method for the problem of a cavity in a layered medium.

be written as:

$$u_i = (u_i)_{[A]} + (u_i)_{[B]} - (u_i)_{[C]}$$
$$\sigma_{ij} = (\sigma_{ij})_{[A]} + (\sigma_{ij})_{[B]} - (\sigma_{ij})_{[C]} \quad (8)$$

For each layer, the solution can be expressed in more detail as:

1. Layer 1 ($y > H$):

$$u_i^{[1]} = (u_i)_{[AU]} + (u_i)_{[BU]} - (u_i)_{[C]}$$
$$\sigma_{ij}^{[1]} = (\sigma_{ij})_{[AU]} + (\sigma_{ij})_{[BU]} - (\sigma_{ij})_{[C]} \quad (9)$$

2. Layer 2 ($H \geq y \geq 0$):

$$u_i^{[2]} = (u_i)_{[AU]} + (u_i)_{[BL]} - (u_i)_{[C]}$$
$$\sigma_{ij}^{[2]} = (\sigma_{ij})_{[AU]} + (\sigma_{ij})_{[BL]} - (\sigma_{ij})_{[C]} \quad (10)$$

3. Layer 3 ($y < 0$):

$$u_i^{[3]} = (u_i)_{[AL]} + (u_i)_{[BL]} - (u_i)_{[C]}$$
$$\sigma_{ij}^{[3]} = (\sigma_{ij})_{[AL]} + (\sigma_{ij})_{[BL]} - (\sigma_{ij})_{[C]} \quad (11)$$

where subscript [A] represents the bonded half-planes with parameters (E_2, ν_2) and (E_3, ν_3), [B] represents the bonded half-planes with parameters (E_1, ν_1) and (E_2, ν_2) and [C] represents the infinite plane with parameters (E_2, ν_2). The additional subscripts U and L represent the solutions for upper and lower half-planes, as the bonded half-planes solutions are different for the upper and lower half-planes.

It is noteworthy that it is difficult, if not impossible, to obtain an analytical solution to the three layer problem. The justification for the scheme is discussed in Appendix A.

3. Numerical implementation

Based on the developed fundamental solution, a solution procedure can be applied to establish the displacement discontinuity method. To demonstrate the solution procedure for the displacement discontinuity method for boundary value problems, a cavity in an infinite layered body is chosen as an example. The cavity is assumed to be very long with its axis parallel to the layers. Therefore, a representative slice perpendicular to the plane of the figure is considered. We can approximate the boundary B of the cavity by N straight line segments joined end to end (see Fig. 4).

For the jth segment, the shear and normal displacement discontinuities applied to this segment are denoted as D_s^j and D_n^j and the actual stresses as σ_s^j and σ_n^j. The actual stresses, σ_s^j and σ_n^j, are induced by the discontinuity values arising on all N segments along the boundary of the cavity. With suitable coordinate transformations to account for the orientations of the line segments, we can express the stresses σ_s^i and σ_n^i ($i = 1$ to N) at suitable collocation points within each segment of curve C. The values of the shear and normal stress components at the ith collocation point can be expressed as

$$\sigma_s^i = \sum_{j=1}^{N} A_{ss}^{ij} D_s^j + \sum_{j=1}^{N} A_{sn}^{ij} D_n^j + P_s^i$$
$$\sigma_n^i = \sum_{j=1}^{N} A_{ns}^{ij} D_s^j + \sum_{j=1}^{N} A_{nn}^{ij} D_n^j + P_n^i \quad (12)$$

where A_{ss}^{ij}, etc., are the boundary stress influence coefficients and P_s^i and P_n^i are the field stress components. The coefficient A_{ss}^{ij}, for example, gives the shear stress at the ith collocation point, σ_s^i, due to a unit applied shear displacement discontinuity at the jth collocation point ($D_s^j = 1$). Introducing prescribed boundary stresses into Eq. (12), we can obtain a system of $2N$ algebraic equations to determine the applied displacement discontinuity D_s^j and D_n^j for $j = 1$ to N. We can then obtain the solutions for other points within the domain since the solutions can be expressed as linear combinations of the displacement discontinuities. The foregoing equations can be used to develop a numerical model for solving two-dimensional boundary value problems. A constant strength element numerical model was first developed and then extended to a

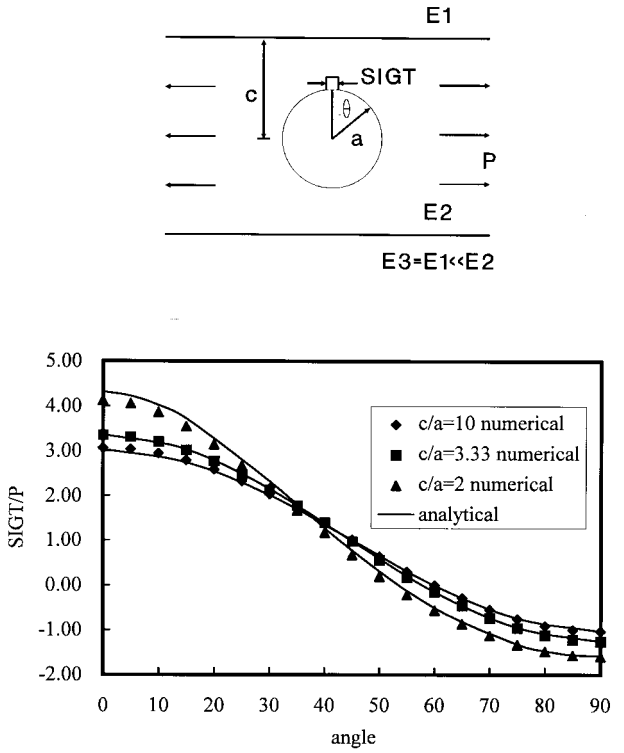

Fig. 5. Tangential stresses along a circular hole in an infinite strip under tension.

more accurate linear element model THREEL, using two internal nodes in each element [14].

4. Verifications

The accuracy of the model is illustrated by comparing the numerical results with the analytical solution for a hole in an infinite strip in tension and with the numerical solution for a pressurized crack within a three-layered system. The results for a circular hole of radius a in a strip of width $2c$ under uniaxial tension are presented in Fig. 5 for different geometric parameter $\lambda = c/a$, where c is the distance from the center of the hole to the surface. The finite strip was simulated by setting E_1 and E_3 to be very small and $E_2 = 50000$ MPa, $\nu_2 = 0.2$. We find that the results are in reasonable agreement with Savin's [17] analytical solution for a finite strip. The relative error is less than 5 % for the 72 element simulation.

As a further check on the solution accuracy a linear variation displacement discontinuity model DIGSMM [18], in which double elements are placed at the bimaterial interfaces to enforce the continuity conditions across the interface(s), is applied for the numerical verification. For completeness, a brief description of this model is given in Appendix B. The numerical results were compared for a pressurized crack within a layer

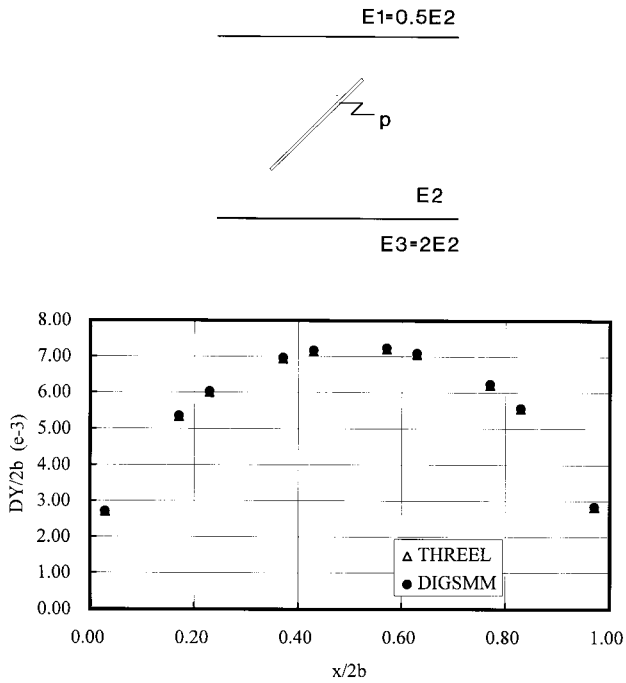

Fig. 6. The closure of a pressurized crack within a three-layered system.

and for a crack crossing an interface ($E_3 = 2E_2 = 4E_1$, $E_2 = 50000$ MPa, internal pressure P = 200 MPa). In the DIGSMM solution 316 additional elements of different sizes were placed on the interfaces. The numerical results in Figs. 6 and 7 are in good agreement with discrepancies of less than 1% for the former case and 3% for the latter case. However, using a Pentium

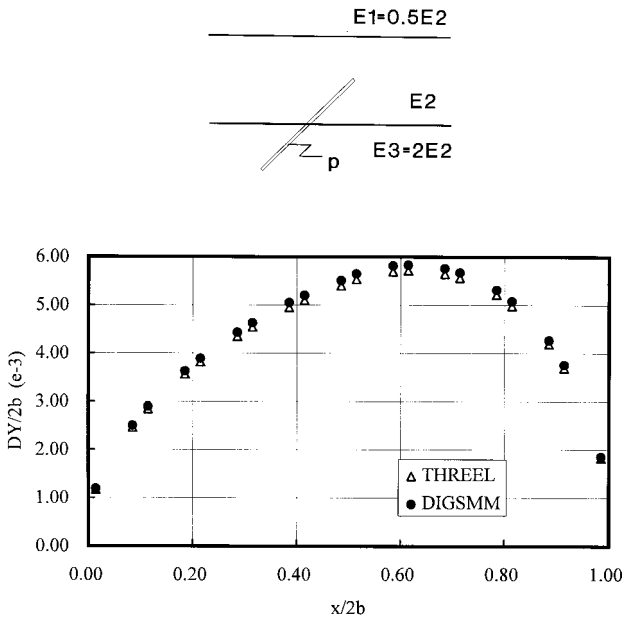

Fig. 7. The closure of a pressurized crack crossing the interface of a three-layered system.

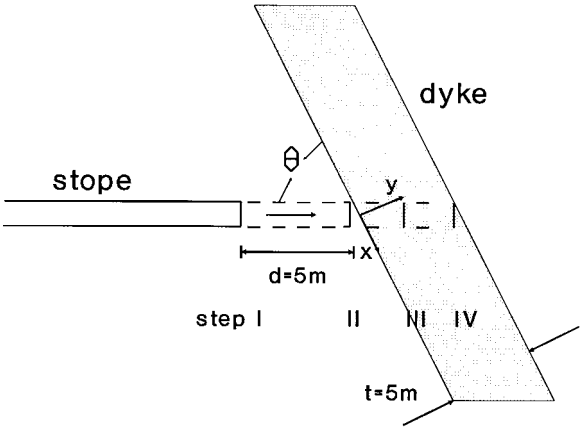

Fig. 8. The problem of a stope approaching a dyke.

II computer, the run time for THREEL (0.06 s) is far less than for DIGSMM (684 s), as the former saves both memory and run time by not using elements along the two interfaces. The explicit interface model would evidently be improved if 'infinite' or other higher order elements were introduced along the interface.

5. Application to mining problems

The orebodies of the Witwatersrand Basin are predominantly associated with sedimentary and minor volcanic rocks [19]. A stope approaching a dyke, with different material properties from the host rock may trigger slip along the interface or may induce stress concentrations within the dyke leading to seismic activity related to rockbursts. An example problem of a stope approaching and penetrating a dyke from different angles (see Fig. 8), with the properties as in Table 1, is analyzed. The approaching angle θ is defined as the angle between the mining direction and the dip direction of the dyke.

The principal stresses along the interface (see Fig. 9a and b) reveal that the difference in the stresses is maximized for the approaching angle nears 60° to 75° which might be related to the maximum sliding also found by York and Dede [20] and the failure mode

Table 1

E (host rock)	78 GPa
ν (host rock)	0.21
E (dyke)	120 GPa
ν (dyke)	0.38
σ_v (vertical in situ stress)	54 MPa
σ_h (horizontal in situ stress)	27 MPa (i.e. k = 0.5)
t (width of dyke)	5 m
d (step I distance from the mining face to dyke)	5 m
θ (angle between the stope and interface)	90°, 75°, 60°, 45°, 30°

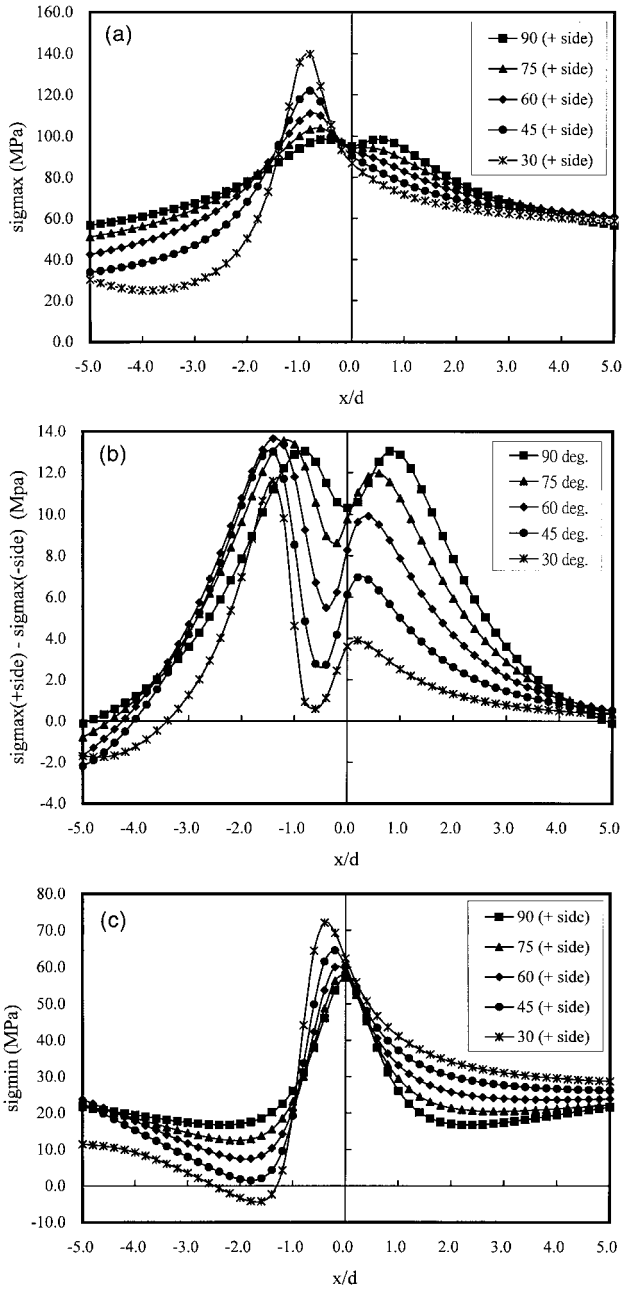

Fig. 9. (a) The influence of approaching angle of stope on the major principal stress along the positive (dyke) side of interface between host rock and dyke. (b) The difference of major principal stress along the interface of host rock and dyke for different approaching angle of stope. (c) The influence of approaching angle of stope on the minor principal stress along the positive (dyke) side of interface between host rock and dyke.

near the interface might change from shear to tensile as the approaching angle gets smaller (see Fig. 9c).

The influence of the contrasting of material properties was also investigated in two sets of simulations, one for different Young's modulus ratios $\rho_E = E_d/E_h$ (E_d for dyke and E_h for host rock, $\nu_d/\nu_h = 1$) and the other for different ratios of Poisson's ratio $\rho_\nu = \nu_d/\nu_h$ (ν_d for dyke and ν_h for host rock, $E_d/E_h = 2$). In both

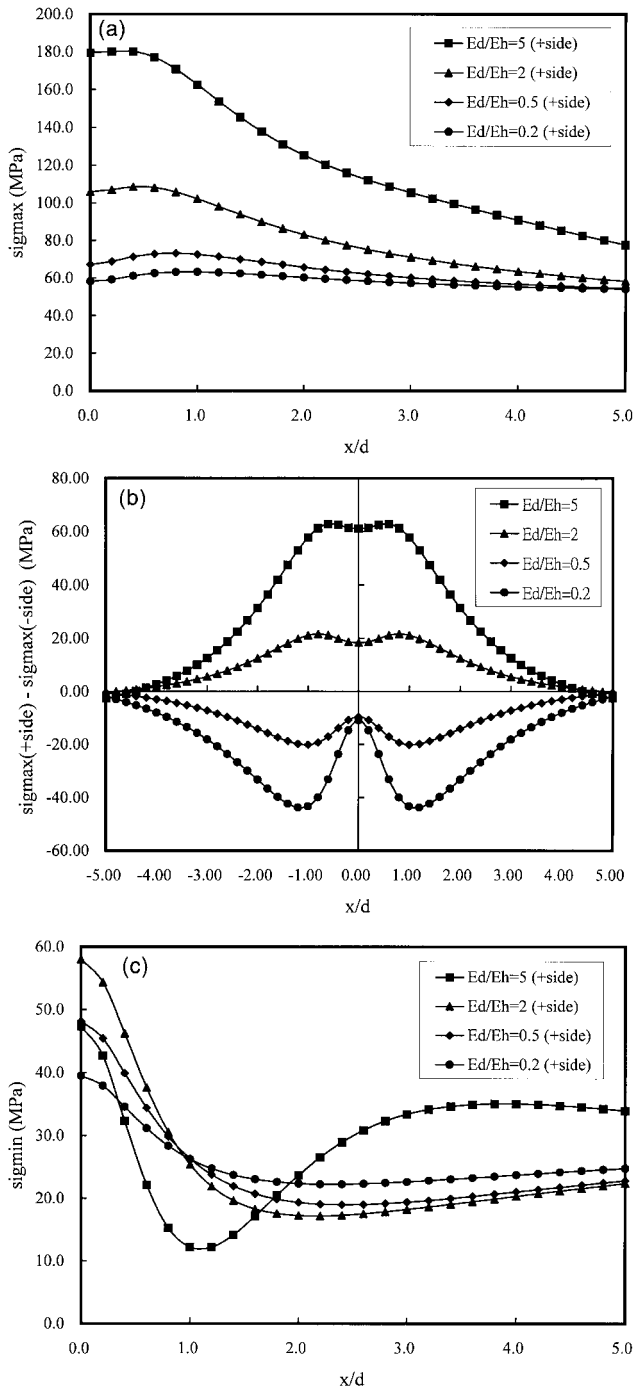

Fig. 10. (a) The influence of Young's modulus ratio E_d/E_h on the major principal stress along the positive (dyke) side of interface between host rock and dyke. (b) The difference of major principal stress along the interface of host rock and dyke for different Young's modulus ratio E_d/E_h. (c) The influence of Young's modulus ratio E_d/E_h on the minor principal stress along the positive (dyke) side of interface between host rock and dyke.

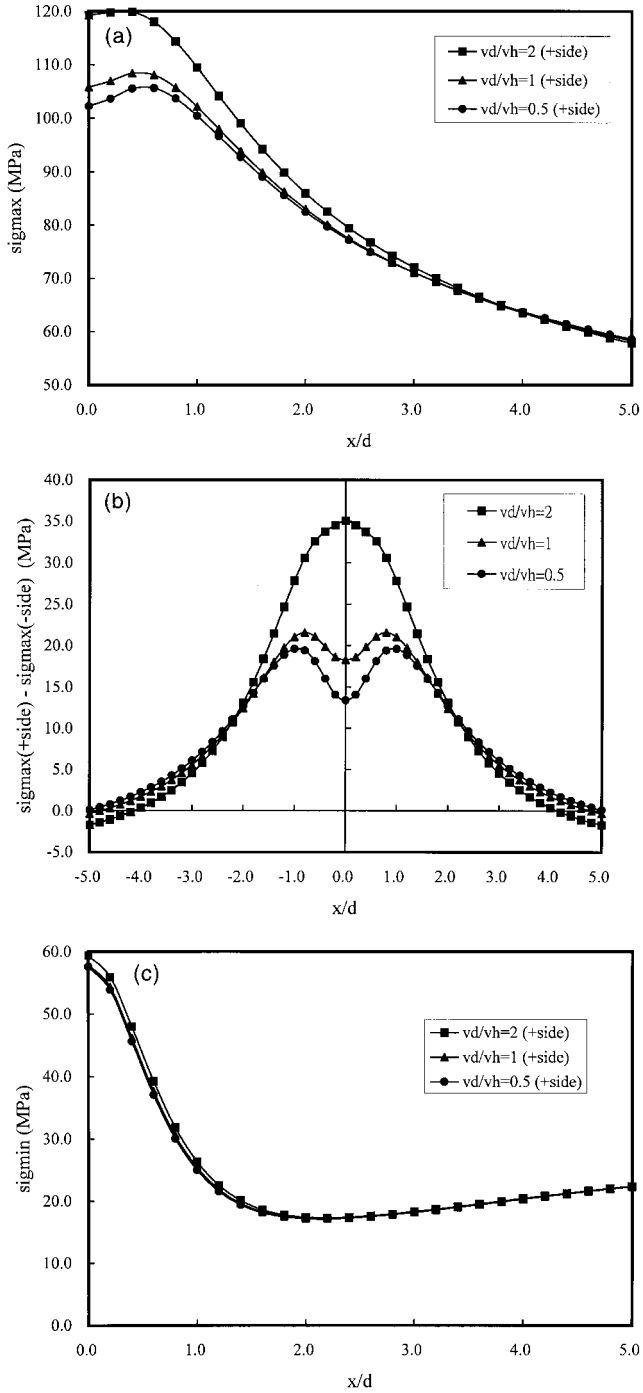

Fig. 11. (a) The influence of the ratio of Poisson's ratio ν_d/ν_h on the major principal stress along the positive (dyke) side of interface between host rock and dyke. (b) The difference of major principal stress along the interface of host rock and dyke for different ratio of Poisson's ratio ν_d/ν_h. (c) The influence of the ratio of Poisson's ratio ν_d/ν_h on the minor principal stress along the positive (dyke) side of interface between host rock and dyke.

sets, we let the distance from the mining face to the first interface of host rock and dyke be $d = 5$ m, the approaching angle be 90°, $E_h = 78$ GPa and $\nu_h = 0.21$. The results in Fig. 10 show that: (1) both the stress concentration and stress difference, between positive and negative sides, increase as ρ_E becomes extreme (larger than 5 or less than 0.2); (2) the stress concentration occurs in the harder, i.e. negative, side and

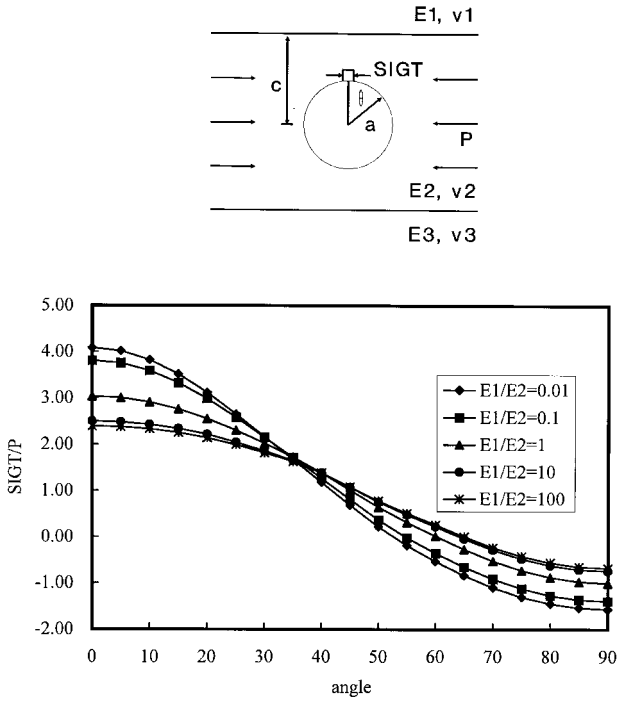

Fig. 12. Tangential stresses along a circular tunnel in a three-layered system (c/a = 2).

shifts from the center by about 1.25 d for a $\rho_E = 0.2$ softer dyke and (3) the case with higher ρ_E possesses higher major principal stress and lower minor principal stress, which illustrates a higher risk of failure. The results in Fig. 11 reveal that the influence of ρ_v on the minor principal stress is not significant and that both the stress concentration and stress difference increase for higher ρ_v.

Using the developed model, a series of analyses, focusing on tunnel problems, was performed. Results of two typical tunnel problems for a three-layered system are given in this paper. For a circular hole in a three-layer medium with $c/a = 2$ and different E_1/E_2 ratios ($E_2 = 50000$ MPa), the results in Fig. 12 show that the softer the outer layer the larger the stress concentration at the crown or invert, and the significant effect for an E_1/E_2 ratio from 0.1 to 10. For a double-tube tunnel, the width d of the pillar between tubes is important. From the numerical solution for different d/a ratios presented in Fig. 13(a) and (b), we can find: (1) a softer outer layer producing greater displacement at the crown or invert more significantly than the sidewall, (2) the displacement is always greater at the pillar sidewall than at the non-pillar sidewall and (3) both of the above effects enlarge when d/a is less than 2.

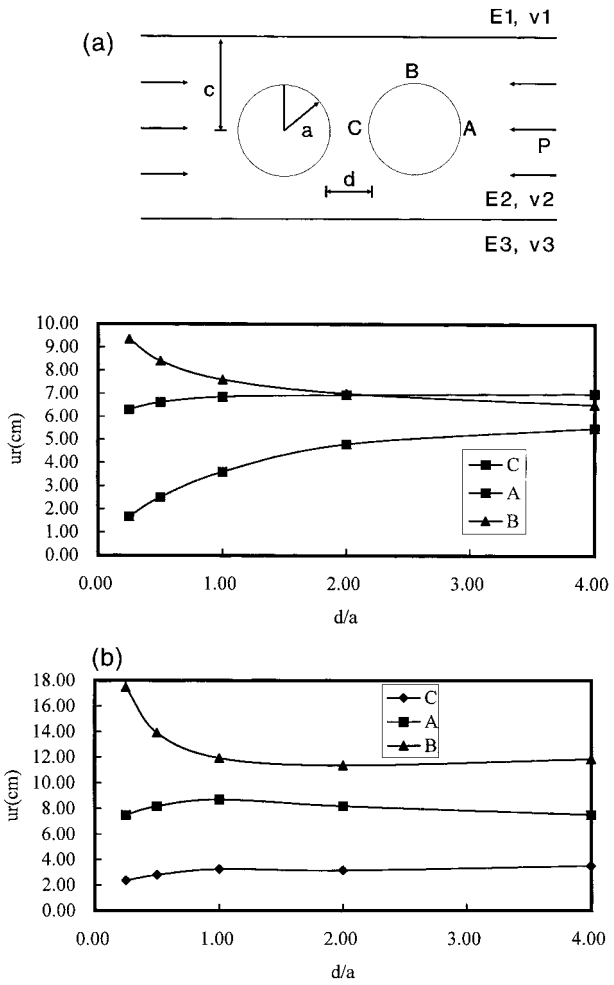

Fig. 13. (a) Radial displacement of a double-tube tunnels for different d/a ratio in a three-layered system ($E_1 = E_2 = E_3$, $c/a = 2$). (b) Radial displacement of a double-tube tunnels for different d/a ratio in a three-layered system ($E_1 = E_3 = 0.1E_2$, $c/a = 2$).

6. Conclusions

The results show that the proposed approach works well in describing the mutual interaction of multiple layers. The boundary element model based on this approach offers a reasonably good numerical solution for the example problems. This is established by comparing the results to both analytic and numerical solutions. The model is capable of analyzing multi-layered systems consisting three layers. The procedure can be intended to treat problems with more than three layers as well as the analysis of three dimensional problems.

The boundary element method presented in this paper also provides reasonable numerical solutions for the example mining problems. The current numerical model THREEL may be suitable for the analysis of fracture propagation, underground excavation and other rock engineering problems in multi-layered rock masses. In certain cases it can be applied to geological inhomogeneity problems such as dyke structures.

Acknowledgements

This work was originally based on the results of the National Science Council Project No. 85-2611-E005-003, Taiwan, by K. Shou, and subsequently formed part of the rockmass behaviour research programme of Rock Engineering, CSIR: Division of Mining Technology. The authors acknowledge the financial assistance and support from the Safety in Mines Research Advisory Committee (SIMRAC).

Appendix A

As a solution for a general three-layer system is not available, a solution from the superposition scheme will be checked for special to general cases:

1. Infinite plane solution:
   An infinite plane can be obtained by letting $E_1 = E_2 = E_3$, which gives the following relation:

$$\begin{aligned} &(u_i)_{[A]} = (u_i)_{[B]} = (u_i)_{[C]} = (u_i)_{[INF]} \\ &(\sigma_{ij})_{[A]} = (\sigma_{ij})_{[B]} = (\sigma_{ij})_{[C]} = (\sigma_{ij})_{[INF]} \end{aligned} \tag{A.1}$$

   where $(u_i)_{[INF]}$ and$(\sigma_{ij})_{[INF]}$ are the infinite plane solutions. Introducing Eq. (A.1) to Eq. (8), we get

$$\begin{aligned} &u_i = (u_i)_{[A]} = (u_i)_{[INF]} \\ &\sigma_{ij} = (\sigma_{ij})_{[A]} = (\sigma_{ij})_{[INF]} \end{aligned} \tag{A.2}$$

2. Half-plane solution:
   Let $E_1 \ll E_2 = E_3$ to simulate a half-plane composed of layers 2 and 3. This setting gives

$$\begin{aligned} &(u_i)_{[A]} = (u_i)_{[HALF]} \\ &(u_i)_{[B]} = (u_i)_{[C]} = (u_i)_{[INF]} \\ &(\sigma_{ij})_{[A]} = (\sigma_{ij})_{[HALF]} \\ &(\sigma_{ij})_{[B]} = (\sigma_{ij})_{[C]} = (\sigma_{ij})_{[INF]} \end{aligned} \tag{A.3}$$

   where $(u_i)_{[HALF]}$ and $(\sigma_{ij})_{[HALF]}$ are the half plane solutions. Introducing Eq. (A.3) to Eq. (8), we get

$$\begin{aligned} &u_i = (u_i)_{[A]} = (u_i)_{[HALF]} \\ &\sigma_{ij} = (\sigma_{ij})_{[A]} = (\sigma_{ij})_{[HALF]} \end{aligned} \tag{A.4}$$

3. Bonded half-planes solution:
   In order to simulate bonded half-planes, we let $E_1 \neq E_2 = E_3$ and obtain the following relation:

$$\begin{aligned} &(u_i)_{[B]} = (u_i)_{[BOND]} \\ &(u_i)_{[A]} = (u_i)_{[C]} = (u_i)_{[INF]} \\ &(\sigma_{ij})_{[B]} = (\sigma_{ij})_{[BOND]} \\ &(\sigma_{ij})_{[A]} = (\sigma_{ij})_{[C]} = (\sigma_{ij})_{[INF]} \end{aligned} \tag{A.5}$$

   where $(u_i)_{[BOND]}$ and $(\sigma_{ij})_{[BOND]}$ are the bonded half-planes solution. Introducing Eq. (A.5) to Eq. (8), we get

$$\begin{aligned} &u_i = (u_i)_{[B]} = (u_i)_{[BOND]} \\ &\sigma_{ij} = (\sigma_{ij})_{[B]} = (\sigma_{ij})_{[BOND]} \end{aligned} \tag{A.6}$$

4. Solution for three-layer system:
   From Eqs. (9)–(11), the solution, layer 2 ($H \geq y \geq 0$) for example, can be expressed as

$$\begin{aligned} &u_i^{[2]} = (u_i)_{[AU]} + (u_i)_{[BL]} - (u_i)_{[C]} \\ &\sigma_{ij}^{[2]} = (\sigma_{ij})_{[AU]} + (\sigma_{ij})_{[BL]} - (\sigma_{ij})_{[C]} \end{aligned} \tag{10a}$$

   in which first and second terms on the right hand side represent the influence of E_2/E_3 and E_1/E_2 interfaces, respectively, and the third term subtracts the 'extra' influence which overlaps the first two terms. Conceptually, it is also necessary to make the conservation of mass. The continuous interfacial conditions are also satisfied automatically, as the stress and displacement are continuous along the interfaces in all of the three terms.

In order to further clarify the interfacial condition, a finite strip case is considered by letting $E_1 = E_3 \ll E_2$ and obtaining the following relation:

$$\begin{aligned} &(u_i)_{[A]} = (u_i)_{[HALF,2]} \qquad (u_i)_{[B]} = (u_i)_{[HALF,1]} \\ &(u_i)_{[C]} = (u_i)_{[INF]} \qquad (\sigma_{ij})_{[A]} = (\sigma_{ij})_{[HALF,2]} \\ &(\sigma_{ij})_{[B]} = (\sigma_{ij})_{[HALF,1]} \qquad (\sigma_{ij})_{[C]} = (\sigma_{ij})_{[INF]} \end{aligned} \tag{A.7}$$

where $(u_i)_{[HALF,1]}$, $(\sigma_{ij})_{[HALF,1]}$, $(u_i)_{[HALF,2]}$ and $(\sigma_{ij})_{[HALF,2]}$ are the half-plane solutions for free surfaces at interface 1 and 2. Looking at the solution, according to Eq.(5), we find

$$\begin{aligned} &(u_i)_{[HALF,2]} = (u_i)_{A} + (u_i)_{I,2} + (u_i)_{S,2} \\ &(u_i)_{[HALF,1]} = (u_i)_{A} + (u_i)_{I,1} + (u_i)_{S,1} \\ &(\sigma_{ij})_{[HALF,2]} = (\sigma_{ij})_{A} + (\sigma_{ij})_{I,2} + (\sigma_{ij})_{S,2} \\ &(\sigma_{ij})_{[HALF,1]} = (\sigma_{ij})_{A} + (\sigma_{ij})_{I,1} + (\sigma_{ij})_{S,1} \end{aligned} \tag{A.8}$$

where sub-indices 1 and 2 refer to the free interface 1 and 2. By introducing Eqs. (A.8) and (A.9) into Eq. (8), the following relation can be obtained for the finite

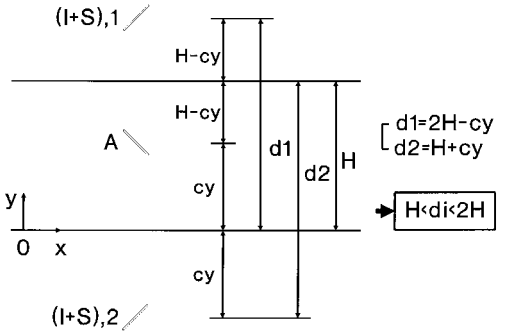

Fig. 14. The influence of (I + S), 1 on interface 2 and the influence of (I + S), 2 on interface 1.

strip problem:

$$u_i = (u_i)_A = [(u_i)_{I,1} + (u_i)_{S,1}] + [(u_i)_{I,2} + (u_i)_{S,2}]$$

$$\sigma_{ij} = (\sigma_{ij})_A + [(\sigma_{ij})_{I,1} + (\sigma_{ij})_{S,1}] + [(\sigma_{ij})_{I,2} + (\sigma_{ij})_{S,2}] \quad \text{(A.9)}$$

Eq. (A.9) reveals that free surface 1 is achieved by sub-index 1 terms and free surface 2 is achieved by sub-index 2 terms. However, the influences of sub-index 2 terms on the interface 1 and the influences of sub-index 1 terms on the interface 2 can be neglected as the influence is equivalent to an element more than thickness H away from the interface. Eq. (A.9) can be illustrated as Fig. (14) in which the influence is equivalent to an element di away from the interface and di $\in (H, 2H)$.

Appendix B

Multiple material regions could be modelled by formulating four additional relationships, for a general two-dimensional problem, to define the interface conditions. These relate to the normal and shear components of the displacement and traction vectors at each point of the interface. To satisfy these interface constraints it is necessary to superimpose two lines of displacement discontinuity elements along each interface, as depicted in Fig. 15.

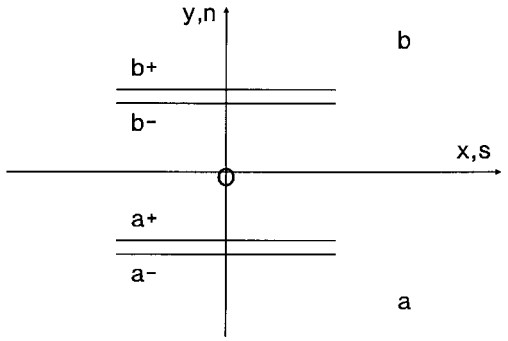

Fig. 15. Superimpose two displacement discontinuity elements along an interface.

Let the unknown displacement discontinuity components in the adjacent elements ***a*** and ***b*** be designated as D_s^a, D_n^a and D_s^b, D_n^b, respectively. For a perfectly bonded interface, the following conditions must be satisfied for displacement components and traction components.

$$U_s^{a-} = U_s^{b+} \qquad U_n^{a-} = U_n^{b+} \qquad \sigma_s^a = \sigma_s^b$$
$$\sigma_n^a = \sigma_n^b \quad \text{(B.1)}$$

The total traction components were expressed in Eq. (12), which can be rewritten in 'self' terms and 'external' terms E_s^i, E_n^i as below:

$$\sigma_s^i = A_{ss}^{ii} D_s^i + [\sum_{\substack{j=1 \\ j\neq 1}}^{N} A_{ss}^{ij} D_s^j + \sum_{j=1}^{N} A_{sn}^{ij} D_n^j + P_s^i]$$
$$= A_{ss}^{ii} D_s^i + E_s^i$$
$$\sigma_n^i = A_{nn}^{ii} D_n^i + [\sum_{\substack{j=1 \\ j\neq i}}^{N} A_{nn}^{ij} D_n^j + \sum_{j=1}^{N} A_{ns}^{ij} D_s^j + P_n^i] \quad \text{(12a)}$$
$$= A_{nn}^{ii} D_n^i + E_n^i$$

Designating the external traction influence components at the point of interest Q as E_s^a, E_s^b, E_n^a, E_n^b, the total traction components at point Q can be written in the form

$$\sigma_s^a = K_a D_s^a + E_s^a \qquad \sigma_n^a = K_a D_n^a + E_n^a$$
$$\sigma_s^b = K_b D_s^b + E_s^b \qquad \sigma_n^b = K_b D_n^b + E_n^b \quad \text{(B.2)}$$

where K_a and K_b are the traction kernel self-effects evaluated using Eq. (2) and the relevant shape functions given by Eq. (4) for region ***a*** (with elastic modulli G_a, ν_a) and ***b*** (with elastic modulli G_b, ν_b), respectively.

Similarly, if F_s^a, F_s^b, F_n^a, F_n^b designate the external displacement influence components at the point of interest Q, the total displacement components on the outer sides of the double element can be written in the form

$$U_s^{a-} = 1/2\ D_s^a + F_s^a \qquad U_n^{a-} = 1/2\ D_n^a + F_n^a$$
$$U_s^{b+} = -1/2\ D_s^b + F_s^b \qquad U_s^{b+} = -1/2\ D_s^b + F_s^b \quad \text{(B.3)}$$

Substituting Eqs. (B.2) and (B.3) into Eq. (B.1), it can be shown that the unknown displacement discontinuities are given by

$$\begin{bmatrix} D_s^a \\ D_n^a \\ D_s^b \\ D_n^b \end{bmatrix} = \frac{1}{K_a + K_b} \begin{bmatrix} K_b & 0 & 1 & 0 \\ 0 & K_b & 0 & 1 \\ K_a & 0 & -1 & 0 \\ 0 & K_a & 0 & -1 \end{bmatrix} \begin{bmatrix} 2(F_s^b - F_s^a) \\ 2(F_n^b - F_n^a) \\ E_s^b - E_s^a \\ E_n^b - E_n^a \end{bmatrix} \tag{B.4}$$

Coupling the above scheme to a general two-dimensional displacement discontinuity method, we can develop the model DIGSMM to simulate the multiple material problems.

References

[1] Banerjee PK, Butterfield R. Boundary element methods in engineering science. London: McGraw-Hill, 1981.

[2] Crouch SL, Starfield AM. Boundary element methods in solid mechanics. London: Allen and Unwin, 1983.

[3] Napier JAL, Ozbay MU. Application of the displacement discontinuity method to the modelling of crack growth around openings in layered media. In: Pasamehmetoglu, editor. Assessment and prevention of failure phenomena in rock engineering. Rotterdam: Balkema, 1993. p. 947–56.

[4] Frasier JT, Rongved L. Force in the plane of two joined semi-infinite plates. J Appl Mech 1957;24:129–74.

[5] Pan E, Amadei B, Kim YI. 2D BEM analysis of anisotropic half-plane problems-application to rock mechanics. Int J Rock Mech Min Sci 1998;35:69–74.

[6] Sneddon IN. Fourier transforms. New York: McGraw-Hill, 1951.

[7] Bufler H. Theory of elasticity of a multilayered medium. J Elast 1971;1:125–43.

[8] Chen WT. Computation of stresses and displacements in a layered elastic medium. Int J Eng Sci 1971;9:775–800.

[9] Wardle LJ. Stress analysis of multi-layered anisotropic elastic systems subject to rectangular loads. CSIRO Aus Div Appl Geomech Tech Paper No. 33, 1980.

[10] Small JC, Booker JR. Finite layer analysis of layered elastic materials using a flexibility approach. Part I: strip loading. Int J Num Methods Eng 1984;20:1025–37.

[11] Benitez FG, Rosakis AJ. Three-dimensional elastostatics of a layer and a layered medium. J Elast 1987;18:3–50.

[12] Shou K. Boundary element method for stress analysis of multi-layered elastic media. J Chin Inst Eng 1994;17:805–14.

[13] Crouch SL. Solution of plane elasticity problems by the displacement discontinuity method. Int J Num Methods Eng 1976;10:301–43.

[14] Crawford AM, Curran JH. Higher-order functional variation displacement discontinuity elements. Int JRock Mech Min Sci Geomech Abstr 1982;19:143–8.

[15] Salamon MDG. Elastic analysis of displacements and stresses induced by mining of seam or reef deposits, Part I. J S Afr Inst Min Metall 1963;64:128–49.

[16] Fung YC. Foundation of solid mechanics. New York: Englewood Cliffs, 1965.

[17] Savin GN. Stress concentration around holes. New York: Pergamon, 1961.

[18] Napier JAL. Internal Report. Johannesburg: Division of Mining Technology, CSIR, 1997.

[19] Schweitzer JK, Johnson RA. Geotechnical classification of deep and ultra-deep Witwatersrand mining areas, South Africa. Miner Deposita 1997;32:335–48.

[20] York G, Dede T. Plane strain numerical modelling of mining induced seismicity through the effects of mine geometry, backfill and dyke material, on tabular reefs at greater depth. In: Gibowicz, Lasocki, editors. Rockbursts and seismicity in mines. Rotterdam: Balkema, 1997. p. 167–72.